Check for updates

Regular Article

Effective exponents near bicritical points

Andrey Kudlis[1,2,a], Amnon Aharony[3,b] , and Ora Entin-Wohlman[3,c]

[1] Abrikosov Center for Theoretical Physics, MIPT, Institutsky Lane, 9, Dolgoprudny 141701, Moscow Region, Russia
[2] ITMO University, Kronverkskiy Prospekt 49, St. Petersburg 197101, Russia
[3] School of Physics and Astronomy, Tel Aviv University, Ramat Aviv, Tel Aviv 6997801, Israel

Abstract The phase diagram of a system with two order parameters, with n_1 and n_2 components, respectively, contains two phases, in which these order parameters are non-zero. Experimentally and numerically, these phases are often separated by a first-order "flop" line, which ends at a bicritical point. For $n = n_1 + n_2 = 3$ and $d = 3$ dimensions (relevant, e.g., to the uniaxial antiferromagnet in a uniform magnetic field), this bicritical point is found to exhibit a crossover from the isotropic n-component universal critical behavior to a fluctuation-driven first-order transition, asymptotically turning into a triple point. Using a novel expansion of the renormalization group recursion relations near the isotropic fixed point, combined with a resummation of the sixth-order diagrammatic expansions of the coefficients in this expansion, we show that the above crossover is slow, explaining the apparently observed second-order transition. However, the effective critical exponents near that transition, which are calculated here, vary strongly as the triple point is approached.

1 Introduction

Phase diagrams involving two competing order parameters, with n_1 and n_2 components, arise in a variety of physical systems. As the temperature is lowered from the disordered phase, one can approach each of these ordered phases, via a phase boundary. These two boundaries meet at a multicritical point, which can be bicritical, tetracritical or triple (Fig. 1) [1–3]. As seen in Fig. 1, the triple point is not really 'critical' or 'multicritical'; however, it is the meeting point of three first-order lines, and it neighbors three phases. It is also reached from the bicritical point. Therefore, we list it together with the 'true' multicritical points. The nature of this multicritical point has been under debate for a long time. in particular, the ϵ−expansions for the renormalization group (RG) fixed points (FPs) corresponding to these multicritical points, and the critical exponents in their close vicinity, have been expanded to fifth order in ϵ and then resummed for estimating their values in three dimensions ($d = 3$). [4] The resulting numbers agreed with those found by other methods, e.g., a resummation of the sixth-order perturbative (divergent) expansions in the original field-theory coefficients at $d = 3$ [5], recent bootstrap calculations [6], Monte Carlo simulations [7] and high-temperature series [8].

All the above calculations derived only the critical exponents *at* the FPs. It turns out that in some cases, the RG flow away from the unstable isotropic FP (see below) is slow, and sometimes it reaches regions far from this FP, with effective critical exponents which are distinct from those calculated *at* that FP. Although such effective exponents were calculated to second order in the coupling constants for the tetracritical point [9], they were not yet calculated for the crossover from bicritical to triple points. In Refs. [11–13], we extended the above calculations, and presented an accurate RG analysis of such systems close to their multicritical points, confirming that for $n = n_1 + n_2 = 3$ in $d = 3$ dimensions, it can either be tetracritical, described by the biconical FP, or a triple point, characterized by a slow RG flow away from the isotropic n−component FP. Since the (stable) biconical FP is very close to the (unstable) isotropic FP, the effective exponents do not change much during the RG flow between them, and the tetracritical point is more or less understood. However, the triple point case requires following the RG trajectory away from the isotropic FP for many RG iterations. Since this flow is very slow, Refs. [11–13] used resummed sixth-order expansions of the derivatives of the $\bar{\beta}$ functions (see below) at the isotropic FP, yielding accurate estimates for the effective exponents, which vary along the RG trajectory. It turned out that the effective exponents change significantly before the triple point is reached. The slow flow indicates that in many

ᵃ e-mail: andrewkudlis@gmail.com
ᵇ e-mail: aaharonyaa@gmail.com (corresponding author)
ᶜ e-mail: orawohlman@gmail.com

3472

Eur. Phys. J. Spec. Top. (2023) 232:3471–3477

cases, the triple point may never be reached, and then one may mistakenly identify the multicritical point as a bicritical one, alas with unusual effective exponents.

As we discuss below, a general four-spin Hamiltonian can be isotropic in spin space, ad it can become anisotropic in many ways. In the description above, the isotropy was broken by the terms which separate the two order parameters, with n_1 and n_2 components. An alternative symmetry breaking is to add a term with cubic symmetry in spin space, $v \sum_{i=1}^{n} S_i^4$. [10] As we discuss below, both anisotropies share the same stability exponent. In Ref. [11] we demonstrated the above RG calculation for the cubic case, and showed that all the RG trajectories approach the same universal line. Some effective critical exponents were then calculated for that case in Ref. [12]. Reference [13] used group theoretical arguments, to show that the universal flow line mentioned above is in fact also reached for the case of $O(1) \bigoplus O(2)$ symmetry, relevant to the multicritical points of interest here. The present paper extends those calculations, by calculating the effective exponents for this case. Qualitatively, the results are similar to those of the cubic case. However, unlike that case, for $2 + 1$ components we need two sets of exponents, $\nu_{\parallel, \perp}$ and $\eta_{\parallel, \perp}$.

1.1 The XXZ case

Most of our results refer to the most ubiquitous example of the uniaxially anisotropic XXZ antiferromagnet in a uniform magnetic field, with $n_1 = 2$, $n_2 = 1$. Other examples are mentioned in Refs. [11, 13]. A uniaxially anisotropic XXZ antiferromagnet has long-range order (staggered magnetization) along its easy axis, Z. A magnetic field $H_{\parallel}$ along that axis causes a spin-flop transition into a phase with order in the transverse plane, plus a small ferromagnetic order along Z. Experiments [14–16] and Monte Carlo simulations on three-dimensional lattices [17–19] typically find an apparent *bicritical* phase diagram in the temperature-field $T - H_{\parallel}$ plane [Fig. 1(a)]: a first-order transition line between the two ordered phases, and two second-order lines between these phases and the disordered (paramagnetic) phase, all meeting at an apparent *bicritical point*.

The field theoretical analysis is based on the Ginzburg–Landau–Wilson (GLW) Hamiltonian density [1], $\mathcal{H}(\mathbf{r}) = \mathcal{H}_0 + U_2 + U_4$, with

$$\mathcal{H}_0(\mathbf{r}) = (\mid \boldsymbol{\nabla} \mathbf{S} \mid^2 + r \mid \mathbf{S} \mid^2)/2, \tag{1}$$

$$U_2 = g[\mid S_{\parallel} \mid^2 - \mid \mathbf{S} \mid^2 /3], \tag{2}$$

$$\begin{aligned} U_4 = u_{\parallel} \mid S_{\parallel} \mid^4 + u_{\perp} \mid \mathbf{S}_{\perp} \mid^4 \\ + 2u_{\times} \mid S_{\parallel} \mid^2 \mid \mathbf{S}_{\perp} \mid^2, \end{aligned} \tag{3}$$

with the local three-component ($n = 3$) staggered magnetization, $\mathbf{S}(\mathbf{r}) \equiv (\mathbf{S}_{\perp}(\mathbf{r}), S_{\parallel}(\mathbf{r}))$. Here, $r = (T - T_c)/T_c$ measures the distance from the critical temperature.

For $g = 0$ and $u_{\parallel} = u_{\perp} = u_{\times} = u$, $\mathcal{H}$ reduces to the isotropic Wilson-Fisher Hamiltonian [20–22], which has an (isotropic) FP at $u = u^{*, I}$.

1.2 Renormalization group

After ℓ iterations of the RG, the size of the system becomes $L \Rightarrow L(\ell) = L/e^{\ell}$, and the correlation length becomes $\xi \Rightarrow \xi(\ell) = \xi/e^{\ell}$ (in units of the lattice constant). In addition, various scaling operators, $\mathcal{O}_a$, e.g., S_i and S_i^2, are rescaled, $\mathcal{O}_a = Z_a(\ell)\mathcal{O}_a$, with scaling factors Z_a which depend on ℓ. [20–22] This maps $\mathcal{H}$ to $\mathcal{H}(\ell)$, with renormalized coefficients, e.g., $r(\ell)$, $g(\ell)$, $u_i(\ell)$. The RG studies the recursion relations which yield the trajectories of these coefficients in the parameter space, and the fixed points of these trajectories.

Using $\xi \sim \mid t \mid^{-\nu}$, where t is the scaling field related to r and ν is the 'isotropic' exponent for the correlation length, we continue iterating until $\min[L(\ell_f), \xi(\ell_f)] = 1$. Thus, ℓ_f is the smaller of $\ln L$ and $-\nu \ln \mid t \mid$. In real or numerical simulations, ℓ_f grows with the system's finite size and/or by the temperature range which is used. At $\ell = \ell_f$, all fluctuations have been eliminated and one can solve the problem using the mean-field Landau theory [21]. Reaching ℓ_f requires the *full RG flow* of the system's Hamiltonian.

The main RG calculations involve the recursion relations for the three coefficients in U_4,

$$\frac{\partial u_i}{\partial \ell} = \bar{\beta}_i[\epsilon, \ u_{\parallel}, \ u_{\perp}, \ u_{\times}]. \tag{4}$$

When $\partial u_i/\partial \ell = 0$, these recursion relations yield four FPs, the Gaussian ($u_{\parallel} = u_{\perp} = u_{\times} = 0$, the isotropic ($u_{\parallel} = u_{\perp} = u_{\times} = u^{*, I}$), the decoupled ($u_{\times} = 0$), and the biconical FPs. In three dimensions, the locations of these fixed points, and the critical exponents in their vicinity, took some time to find, mainly because of difficulties to extrapolate the recursion relations down from $d = 4$ to $d = 3$, given as divergent series in $\epsilon = 4 - d$ and in the u's. One way to overcome this is to use resummation techniques, e.g., by taking into account the singularities of the series' Borel transforms [4], and extrapolating the results to $\epsilon = 1$. These showed that for $n = d = 3$ the only stable FP is the biconical one, which is very close to the unstable isotropic one. The results for the critical exponents agreed with a resummation of the sixth-order perturbative (divergent) expansions in the original field-theory coefficients at $d = 3$ [5], with recent bootstrap calculations [6], with Monte Carlo simulations [7] and with high-temperature series [8].

Since the biconical and isotropic FPs are very close to each other, we decided to study in detail the recursion relations in the vicinity of the isotropic FP. To first order in the us, we need the three exponents of its stability in the space of the us. It turns out that the associated eigenvectors of these recursion relations are given by group theory. In our case, $[O(n) \Rightarrow O(n_1) \bigoplus O(n_2)]$, group theory shows that these eigen-operators are [4,
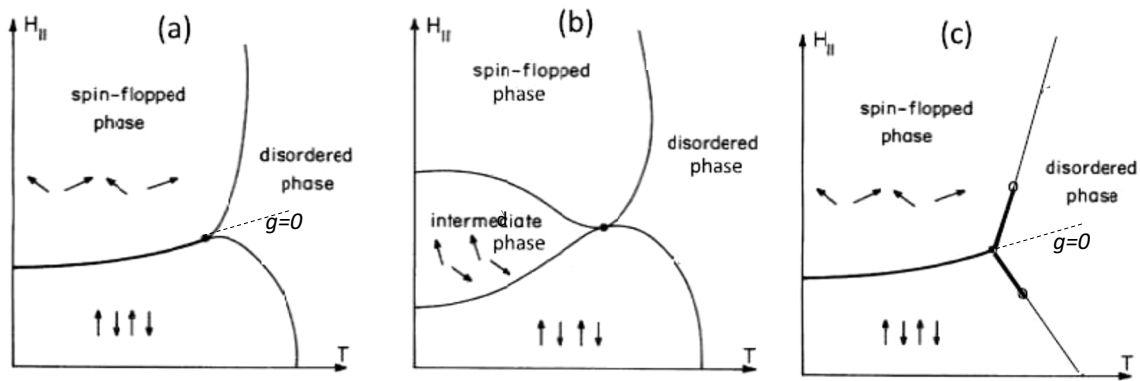
Fig. 1 Possible phase diagrams for the XXZ antiferromagnet in a longitudinal magnetic field. **a** Bicritical phase diagram. **b** Tetracritical phase diagram. **c** Diagram with a triple point. Thick lines—first-order transitions. Thin lines—second-order transitions. The first-order transition lines between the ordered phases and the disordered paramagnetic phase turn into second-order ones at tricritical points (small empty circles). After Refs. [2, 3]

7, 23–25]

$$\mathcal{P}_{4,0} \equiv \mid \mathbf{S} \mid^4, \quad \mathcal{P}_{4,2} \equiv \mid \mathbf{S} \mid^4 [x - n_1/n],$$
$$\mathcal{P}_{4,4} \equiv \mid \mathbf{S} \mid^4 \big[\frac{n_1 n_2}{(n+2)(n+4)}$$
$$+ x(1-x) - \frac{n_1(1-x) + n_2 x}{n+4} \big], \quad (5)$$

where $x = S_\parallel^2 / \mid \mathbf{S} \mid^2$. For $n = 3 = 2 + 1$, the corresponding stability exponents (agreed by all the extrapolations) are [6]

$$\lambda_0 \approx -0.78, \quad \lambda_2 \approx -0.55, \quad \lambda_4 \approx 0.01. \quad (6)$$

Rewriting Eq. (3) as

$$U_4 = (u^{*,I} + p_0)\mathcal{P}_{4,0} + p_2 \mathcal{P}_{4,2}$$
$$- p_4 \mathcal{P}_{4,4}, \quad (7)$$

the linear recursion relations for the coefficients p_i and their solutions are

$$dp_i/d\ell \approx \lambda_i p_i \quad \Rightarrow \quad p_i(\ell) = p_i(0)e^{\lambda_i \ell},$$
$$i = 0, \ 2, \ 4. \quad (8)$$

Group theory also identifies the eigenvectors, which yield the exact relations

$$\delta u_\parallel = p_0 + (70p_2 + 24p_4)/105,$$
$$\delta u_\perp = p_0 - (35p_2 - 9p_4)/105,$$
$$\delta u_\times = p_0 + (35p_2 - 72p_4)/210, \quad (9)$$

where $\delta u_i = u_i - u^{*,I}$, $i = \parallel, \ \perp, \ \times$. These linear expressions can easily be generalized to any n_1 and n_2.

The largest (negative) exponent λ_0 corresponds to the stability within the $O(3)$−symmetric case, $\mathcal{P}_{4,0}$. In our case, the exponent λ_2 corresponds to a term which splits the $O(3)$ isotropic symmetry group into $O(1) \bigoplus O(2)$. Similar to U_2, $\mathcal{P}_{4,2}$ 'prefers' ordering of $S_\parallel$ or of $\mathbf{S}_\perp$. At the multicritical point, the $O(3)$ symmetry must be preserved, and therefore below we set $p_2 = 0$.

Since $\lambda_4 > 0$, the isotropic FP is unstable at $d = 3$, and the small $\lambda_4 > 0$ represents the slow crossover away from the isotropic FP. Examples of the flow trajectories in the $p_0 - p_4$ are show in Fig. 2. For some range of the parameters, the RG flow reaches slowly the less symmetric FP (biconical or cubic), and the bicritical phase diagram should be replaced by the tetracritical diagram [26]. Alternatively, the iterations first flow slowly and remain near the isotropic FP, and then flow quickly towards the triple point, beyond which the transition becomes fluctuation-driven first order. Neither of these agrees with the experiments or the simulations.

Indeed, the same value of λ_4 was also found for the crossover from the isotropic to the cubic FP [5–7, 10, 11, 27, 28]. In fact, the most general space of even quartic terms contains fifteen coefficients u_{abcd}, which split into groups of $1 + 5 + 9$. All the coefficients in each group have the same stability exponent. The cubic v and our p_4 both belong the the group of size 9, and therefore their qualitative behavior is similar.

2 Our calculation

Expanding Eq. (4) to second order in the deviations from the isotropic FP,

$$\frac{\partial u_i}{\partial \ell} = \sum C_{abc} L_{abc}^i (\delta u_\parallel)^a (\delta u_\perp)^b (\delta u_\times)^c, \quad (10)$$

with the integers $a, b, c = 0, 1, 2$, $1 \le a + b + c \le 2$, $C_{abc} = (\delta_{a2} + \delta_{b2} + \delta_{c2})/2$, and e.g.,

$$L_{100}^i = \text{Resum} \Big[\frac{\partial \bar{\beta}_i}{\partial u_\parallel} \Big]_{\{u_j = u^{*,I}\}},$$

$$L^i_{011} = \mathrm{Resum}\left[\frac{\partial^2 \bar{\beta}_i}{\partial u_\perp \partial u_\times}\right]_{\{u_j = u^{*,I}\}},$$

$$L^i_{020} = \mathrm{Resum}\left[\frac{\partial^2 \bar{\beta}_i}{\partial (u_\perp)^2}\right]_{\{u_j = u^{*,I}\}}. \qquad (11)$$

The derivatives are calculated at the isotropic FP. Using the known ϵ-expansion of $u^{*,I}$, they are obtained as sixth order polynomials in ϵ, which are then resummed—using the methods explained, e.g., in Ref. [11]. The resulting values are listed in the Supplementary Material [29].

Diagonalizing the 3×3 matrix of the linear terms in Eq. (10), we recover Eq. (8). The resulting numerical values of the eigenvalues λ_is, are found to be very close to the numbers in Eq. (6), which was based on the full sixth-order recursion relations and on other accurate calculations. Also, the eigenvectors turn out to be very close to the exact Eq. (5). We next use Eq. (9) to replace Eq. (10) by quadratic equations for the ps. As stated above, at the multicritical point, we set $g = 0$ and $p_2 = 0$. In this case, we are left with the RG flow in the $p_0 - p_4$ plane, and we generalize the calculation of Ref. [11]. We first replace p_0 by the nonlinear scaling field q_0, which obeys

$$dq_0/d\ell \approx \lambda_0 q_0 \;\Rightarrow\; q_0(\ell) = q_0(0)e^{\lambda_0 \ell} \qquad (12)$$

to all orders in the ps. This is achieved by writing

$$q_0 = p_0 + z_{20}p_0^2 + z_{11}p_0 p_4 + z_{02}p_4^2 + \dots, \qquad (13)$$

and choosing the zs so that the higher-order coefficients in $dq_0/d\ell$ vanish [29]. Substituting Eq. (12) into $dp_4/d\ell$, we find

$$\frac{dp_4}{d\ell} = \lambda_4 p_4 + A\lambda_0 q_0(\ell)p_4 - Bp_4^2, \qquad (14)$$

where $B = 0.144(11)$ and $A = 2.369(67)$. [29] Rewriting this as a differential equation in $1/p_4$, writing $x = e^{\lambda_0 \ell}$ and $1/p_4(x) = e^{-Ax}x^{-\lambda_4/\lambda_0}W(x)$, yields

$$dW/dx = [B/\lambda_0]e^{\tilde{A}x}x^{\lambda_4/\lambda_0 - 1}, \qquad (15)$$

with the solution

$$W(\ell) = \frac{e^{\tilde{A}}}{p_4(0)} + \frac{(-\tilde{A})^{-\lambda_4/\lambda_0}B}{\lambda_0} \times$$
$$\left(\Gamma[\lambda_4/\lambda_0, -\tilde{A}] - \Gamma[\lambda_4/\lambda_0, -\tilde{A}e^{\lambda_0 \ell}]\right), \qquad (16)$$

where $\tilde{A} = Aq_0(0)$, and $\Gamma[s, z]$ is the incomplete gamma function. From Eq. (13), the quadratic approximation gives

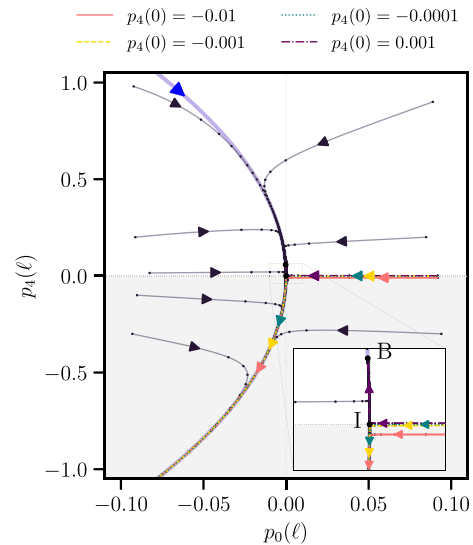$$p_0 \approx q_0 - z_{20}q_0^2 - z_{11}q_0 p_4 - z_{02}p_4^2. \qquad (17)$$

Fig. 2 Flow trajectories in the $p_0 - p_4$ plane for several initial points. Four of them (presented within the legend bar) are used as initial points for analysis of effective exponents. The trajectories are constructed on the basis of Eqs. (17) and (16). The dots indicate integer values of ℓ. The blue thick line is the universal asymptotic line, when $q_0 = 0$. The letters B and I correspond to the biconical and isotropic $(p_4^{*,I} = 0)$ fixed points, respectively

This equation, together with Eqs. (12) and (16), generates the trajectories in the $p_0 - p_4$ plane, shown in Fig. 2.

For large ℓ, $x = e^{\lambda_0 \ell}$ is small, and $\Gamma[s, z] = -z^s/s + \mathcal{O}[1]$, so that $\Gamma[\lambda_4/\lambda_0, -Ax] \propto e^{\lambda_4 \ell}$. This result can be obtained directly: For $\ell > \ell_1$ we can neglect $q_0(\ell)$ in Eq. (14). The solution to this equation is then

$$p_4(\ell) = \frac{p_4(\ell_1)e^{\lambda_4(\ell - \ell_1)}}{1 + Bp_4(\ell_1)[e^{\lambda_4(\ell - \ell_1)} - 1]/\lambda_4}. \qquad (18)$$

Indeed, this dependence of p_4 on ℓ is approached for all $p_0(0)$ and large ℓ. The corresponding asymptotic line, given by $q_0 = 0$, depends only on the coefficients z_{ab} in Eq. (13) and on B. Since these numbers all follow from the derivatives of the $\bar{\beta}$-functions at the isotropic FP, they are all *universal*. Therefore, the asymptotic line is also universal.

Since λ_4 is very small, the variation of the second term in the denominator with ℓ is slow. In our case, $B > 0$, implying a slow variation in $p_4(\ell)$ for positive p_4, approaching the biconical FP $p_4^{*,B} = \lambda_4/B = 0.057(51)$. This value of $p_4^{*,B}$ agrees with the full solution of the original sixth order recursion relations, justifying our quadratic approximation. In contrast, for $p_4(0) < 0$, $p_4(\ell)$ becomes more and more negative. At first, it decreases slowly, not far from the isotropic FP, but when $e^{\lambda_4 \ell}$ becomes of order unity, this decrease becomes faster (the points at integer ℓ become less dense), and $p_4(\ell)$ diverges at $\ell = \ell_2$, when $[e^{\lambda_4(\ell_2 - \ell_1)} - 1]/\lambda_4 \approx (\ell_2 - \ell_1) = -1/[Bp_4(\ell_1)]$. This
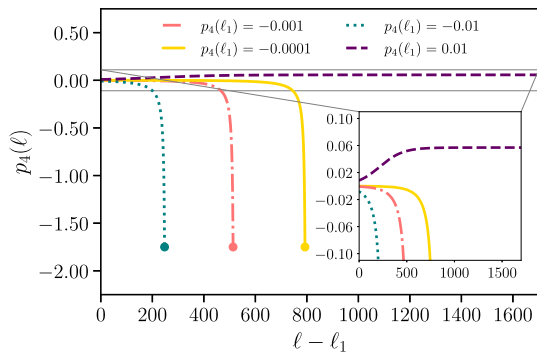
Fig. 3 The function $p_4(\ell)$, Eq. (18) for $B = 0.144$, $\lambda_4 = 0.0082$, $q_0(\ell_1) = 0$ and different $p_4(\ell_1)$, especially highlighted in the flow diagram. Thick dots correspond to the values of ℓ, when the corresponding $p_4 = -35u^{*,I}/8 = -1.75$. At this (approximate) point, the transition becomes first order and the bicritical point becomes a triple point

value is larger for smaller $| p_4(\ell_1) |$ [and, therefore, also for smaller $| p_4(0) |$]. Within our quadratic approximation, we are not allowed to follow this solution beyond some finite value, say $p_4 < -.8$. Although Figs. 2 and 3 show larger values of $| p_4(\ell) |$, those parts can only be take qualitatively; it is reasonable that a full solution will also continue downwards, on the asymptotic trajectory.

For large ℓ, away from criticality $(T \neq T_c)$, we can neglect $p_0(\ell)$ and approximate the free energy by its Landau expression,

$$F = r(\ell) \mid \mathbf{S} \mid^2 /2 + \mid \mathbf{S} \mid^4 (u^{*,I} - p_4(\ell)[2/35 + x(1-x) - (1+x)/7]). \qquad (19)$$

For $p_4(\ell) < 0$, the last term in minimal at $x = 1$, when the square brackets become $-8/35$. However, the total quartic term becomes negative when $p_4 = -35u^{*,I}/8 \approx -1.75$, and then the transition becomes first order, identifying the triple point. Interestingly, this is exactly the same value found for the cubic case [11].

3 Effective critical exponents

So far, we discussed only the recursion relations for the quartic spin terms, U_4. To obtain the physically measurable critical exponents we now return to the quadratic terms, which contain $r(\ell)$ and $g(\ell)$. Although these are the correct linear scaling fields, it is also convenient to write the quadratic terms as

$$(\mid \boldsymbol{\nabla} \mathbf{S} \mid^2 + r_\parallel \mid S_\parallel \mid^2 + r_\perp \mid \mathbf{S}_\perp \mid^2)/2, \qquad (20)$$

where $r_\parallel = r - n_1 g$ and $r_\perp = r + n_2 g$ are the temperature parameters associated with the spins $S_\parallel$ and $\mathbf{S}_\perp$.

At the isotropic FP, $g = 0$, and the two r's have the same recursion relation. However, these relations

change at order u_i^2,   [1, 4, 9]

$$\partial r_i/\partial\ell = (2 - \eta_i)r_i + O[\{u_i\}]. \qquad (21)$$

The different prefactors of the first terms result from the different rescaling factors of the operators $S_\parallel^2$ and $\mid \mathbf{S}_\perp \mid^2$, with $\eta_i = O[u_i^2]$. Technically, these are obtained from keeping the coefficient of the gradient term equal to 1.

The η_is describe the power law decay of the correlation functions at T_c. Generally, the Fourier transform of the two point correlation function, $G_{ii}(\mathbf{q}) \equiv \langle S_i(\mathbf{q})q)S_i(-\mathbf{q})\rangle$, obeys the generalized scaling relation [30, 31]

$$G_{ii}(t, \mathbf{q}) = e^{(2-\eta_i)\ell}G_{ii}(e^{\ell/\nu}t, \\ e^{\ell\phi/\nu}g, \ e^\ell\mathbf{q}), \qquad (22)$$

where $i = \parallel$ or $\perp$. Here, t and g are the nonlinear scaling fields related to r and g. Note: the exponent ν is still isotropic; there is only one correlation length at the multicritical point. All the other critical exponents can be derived from these exponents, e.g., $\gamma_i = (2 - \eta_i)\nu$ (obtained from $G_{ii}(t, 0) \sim t^{-\gamma_i}$) and $\alpha = 2 - d\nu$. The exponent ϕ is the crossover exponent connected with the flow away from the multicritical point towards positive or negative g (upper or lower phases in Fig. 1. All the effective exponents $1/\nu$, ϕ/ν, $\eta_\parallel$ and $\eta_\perp$ can be derived from the recursion relations of the two-points correlation functions. [32] As before, we expand the corresponding renormalization factors in powers of ϵ and the p_is, express the coefficients in terms of $u^{*,I}$ and resum these sixth-order ϵ−expansions to obtain expansions of these four exponents to second order in the p_i.

Given the solutions $p_i(\ell)$ from the previous section, we have derived the four effective exponents as functions of ℓ. The effective exponents are given by

$$\chi_i = \chi_{00}^i + \chi_{10}^i q_0 + \chi_{20}^i q_0^2 + \chi_{01}^i p_4 \\ + \chi_{11}^i q_0 p_4 + \chi_{02}^i p_4^2, \qquad (23)$$

where $\chi_i = \nu$, ϕ and $\eta_{\parallel, \perp}$. The coefficients are presented in Table 1, and the results are plotted in Fig. 4. Due to our quadratic approximations, these plots stop at $p_4(\ell) = -.8$. However, the qualitative large variations are expected to continue towards the triple point.

Note: For the small initial values of p_4, all the exponents stay close to their isotropic FP values for a large range of ℓ. This may explain the experimental and numerical observed results. However, as the correlation length increases the effective exponents deviate strongly from their isotropic values, until eventually the transition becomes first order at the triple point. Also, at the isotropic FP, we must have $\eta_\parallel = \eta_\perp$, and indeed $\eta_{00}^\parallel = \eta_{00}^\perp$. Interestingly, $\eta_{02}^\parallel$ and $\eta_{02}^\perp$ have opposite signs. Since these terms dominate at large ℓ, the deviation between the two η's increases as the triple point is approached
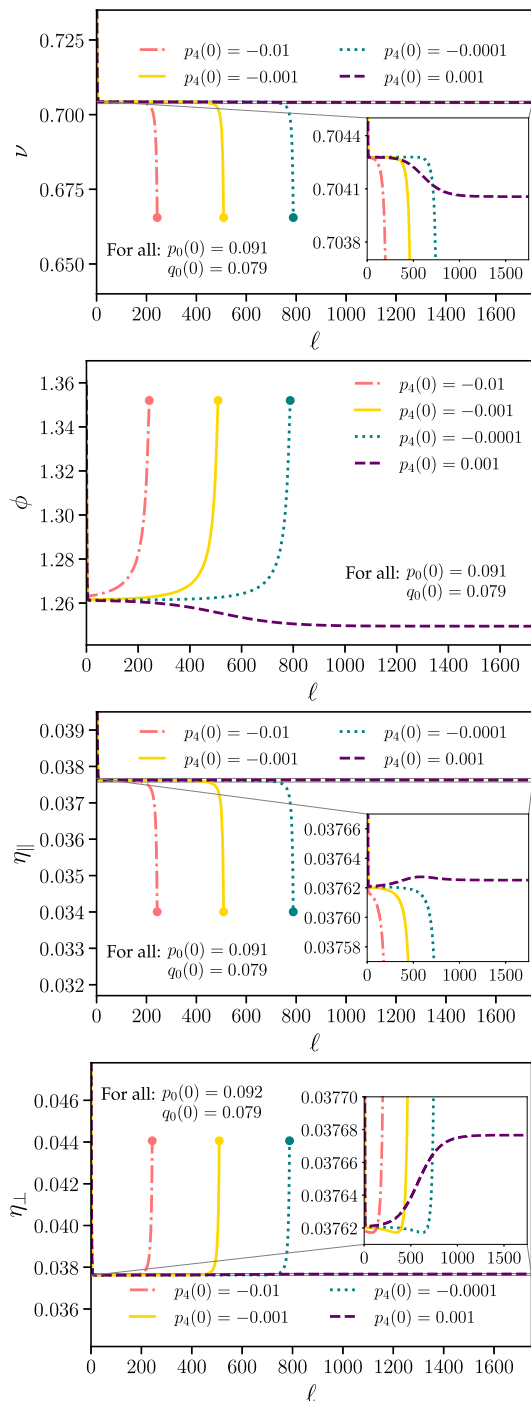
3476

Eur. Phys. J. Spec. Top. (2023) 232:3471–3477

Fig. 4 Dependence of effective critical exponents ν, ϕ, $\eta_\parallel$, and $\eta_\perp$ on the RG flow parameter ℓ, based on the four colored trajectories in Fig. 2. Different lines correspond to different initial values $p_4(0)$ and $p_0(0)$. Due to our quadratic approximation, all the plots stop at $p_4(\ell) = -.8$

Table 1 Numerical values of coefficients entering Eq. (23)

Coeff.	Value	Coeff.	Value
ν_{00}	0.70428(76)	$\eta_{00}^{\parallel}$	0.03762(85)
ν_{10}	0.731(10)	$\eta_{10}^{\parallel}$	0.1914(22)
ν_{01}	−0.0004(16)	$\eta_{01}^{\parallel}$	0.00038(22)
ν_{11}	−0.0009(69)	$\eta_{11}^{\parallel}$	−0.0081(32)
ν_{20}	2.369(61)	$\eta_{20}^{\parallel}$	0.630(18)
ν_{02}	−0.0610(24)	$\eta_{02}^{\parallel}$	−0.00517(70)
ϕ_{00}	1.2614(16)	$\eta_{00}^{\perp}$	0.03762(85)
ϕ_{10}	0.983(16)	$\eta_{10}^{\perp}$	0.1942(27)
ϕ_{01}	−0.2021(39)	$\eta_{01}^{\perp}$	0.00038(63)
ϕ_{11}	−0.203(12)	$\eta_{11}^{\perp}$	−0.0033(87)
ϕ_{20}	3.314(83)	$\eta_{20}^{\perp}$	0.684(20)
ϕ_{02}	−0.1110(34)	$\eta_{02}^{\perp}$	0.0106(14)

4 Conclusions

Our accurate renormalization group calculations in the vicinity of the isotropic fixed point show that for a range of parameters, when $p_4(0) < 0$, the asymptotic multicritical point for the $n = 2 + 1$ order parameters must cross over from the isotropic FP behavior to the triple point and the fluctuation-driven first-order transition. Our calculated flow trajectories also allow us to calculate the effective critical exponents, which remain close to their isotropic values for a range of system sizes or correlation lengths, but then show large deviations as these length grow larger. Our results are qualitatively similar to those found for the cubic case, [11] and must also describe many other apparent bicritical points. [13]

References

1. J.M. Kosterlitz, D.R. Nelson, M.E. Fisher, Bicritical and tetracritical points in anisotropic antiferromagnetic systems. Phys. Rev. B **13**, 412 (1976)
2. A.D. Bruce, A. Aharony, Coupled order parameters, symmetry-breaking irrelevant scaling fields, and tetracritical points. Phys. Rev. B **11**, 478 (1975)
3. E. Domany, D. Mukamel, M.E. Fisher, Destruction of first-order transitions by symmetry-breaking fields. Phys. Rev. B **15**, 5432 (1977)
4. P. Calabrese, A. Pelissetto, E. Vicari, Multicritical phenomena in $O(n_1) \bigoplus O(n_2)$-symmetric theories. Phys. Rev. B **67**, 054505 (2003)
5. J.M. Carmona, A. Pelissato, E. Vicari, N-Component Ginzburg-Landau Hamiltonians with cubic anisotropy: A six-loop study. Phys. Rev. B **61**, 15136 (2000)
6. S. M. Chester, W. Landry, J. Liu, D. Poland, D. Simmons-Duffin, N. Su, A. Vichi, Bootstrapping Heisenberg magnets and their cubic anisotropy. Phys. Rev. D **104**, 105013 (2021). This paper contains an updated table of the exponents
7. M. Hasenbusch, E. Vicari, Anisotropic perturbations in three-dimensional O(N)-symmetric vector models. Phys. Rev. B **84**, 125136 (2011)
8. P. Butera, M. Comi, Renormalized couplings and scaling correction amplitudes in the N-vector spin models on the sc and the bcc lattices. Phys. Rev. B **58**, 11552 (1998)
9. R. Folk, Y. Holovatch, G. Moser, Field theory of bicritical and tetracritical points. I. Statics. Phys. Rev. E **78**, 041124 (2008)
10. A. Aharony, Critical behavior of anisotropic cubic systems. Phys. Rev. B **8**, 4270 (1973)
11. A. Aharony, O. Entin-Wohlman, A. Kudlis, Different critical behaviors in cubic to trigonal and tetragonal perovskites. Phys. Rev. B **105**, 104101 (2022)
12. A. Aharony, O. Entin-Wohlman and A. Kudlis, *Bi- and Tetracritical phase diagrams in three dimensions*, Low Temp. Phys. **48**, 483 (2022) [Fiz. Niz. Temp. (Kharkov) **44**, 542 (2022)]
13. A. Aharony, O. Entin-Wohlman, Puzzle of bicriticality in the XXZ antiferromagnet. Phys. Rev. B **106**, 094424 (2022)
14. A.R. King, H. Rohrer, Spin-flop bicritical point in MnF_2. Phys. Rev. B **19**, 5864 (1979)
15. For a review, see Y. Shapira, Experimental Studies of Bicritical Points in 3D Antiferromagnets, in R. Pynn and A. Skjeltorp, eds., **Multicritical Phenomena**, Proc. NATO advanced Study Institute series B, Physics; Vol. 6, Plenum Press, NY, p. 35 (1984)
16. Y. Shapira, Phase diagrams of pure and diluted low" anisotropy antiferromagnets: Crossover effects (invited). J. Appl. Phys. **57**, 3268 (1985)
17. W. Selke, M. Holtschneider, R. Leidl, S. Wessel, G. Bannasch, Uniaxially anisotropic antiferromagnets in a field along the easy axis. Phys. Procedia **6**, 84–94 (2010)
18. G. Bannasch, W. Selke, Heisenberg antiferromagnets with uniaxial exchange and cubic anisotropies in a field. Eur. Phys. J. B **69**, 439 (2009)
19. J. Xu, S.-H. Tsai, D.P. Landau, K. Binder, Finite-size scaling for a first-order transition where a continuous symmetry is broken: The spin-flop transition in the three-dimensional XXZ Heisenberg antiferromagnet. Phys. Rev. E **99**, 023309 (2019)
20. K.G. Wilson, The RG and critical phenomena (1982, Nobel Prize Lecture). Rev. Mod. Phys. **55**, 583 (1983)
21. M.E. Fisher, Renormalization group theory: its basis and formulation in statistical physics. Rev. Mod. Phys. **70**, 653 (1998)
22. C. Domb, M.S. Green (eds.), *Phase Transitions and Critical Phenomena*, vol. 6 (Academic Press, NY, 1976)
23. F. J. Wegner, Critical Exponents in Isotropic Spin Systems. Phys. Rev. B **6**, 1891 (1972). See also F. J. Wegner, *The critical state, General Aspects*, in Ref. [22], p. 7
24. A. Codello, M. Safari, G. P. Vacca, and O. Zanusso, Critical models with $n \leq 4$ scalars in $d = 4 - \epsilon$, Phys. Rev. D **102**, 065017 and references therein (2020)
25. A. Pelissetto, E. Vicari, Critical phenomena and renormalization-group theory. Phys. Rep. **368**, 542 (2002)
26. For $n > 3$ the stable FP is the decoupled one, which also implies a tetracritical phase diagram: A. Aharony, *Comment onrbitrary "Bicritical and Tetracritical Phenomena and Scaling Properties of the SO(5) Theory"*, Phys. Rev. Lett. **88**, 059703 and references therein. See also Ref. [27] (2002)
27. A. Aharony, *Dependence of universal critical behavior on symmetry and range of interaction*, in Ref. [22], p. 357
28. L.T. Adzhemyan, E.V. Ivanova, M.V. Kompaniets, A. Kudlis, A.I. Sokolov, Six-loop ϵ expansion study of three-dimensional n-vector model with cubic anisotropy. Nucl. Phys. B **940**, 332 (2019)
29. A full list of the numbers can be foud i the "ancillarey files" on arXiv:2304.08265
30. M.E. Fisher, A. Aharony, Scaling function for critical scattering. Phys. Rev. Lett. **31**, 1238 (1973)
31. M. E. Fisher, A. Aharony, Scaling function for two point correlations, I. Epsilon expansion near 4 dimensions. Phys. Rev. B**10**, 2818 (1974)
32. Instead of following the original RG calculations, [30] here we extended the field theoretical calculations of Refs.. [4] and [9], to sixth order in ϵ. Using their definitions, we calculated the operator reccale factors for S_i ad S_i^2 as series in the u_i's, and derived from them the corrsponding resummed coefficients for the quadratic expansions of the various exponents near the isotropic FP